JACS
JOURNAL OF THE AMERICAN CHEMICAL SOCIETY

Communication

pubs.acs.org/JACS

Macromolecularly "Caged" Carbon Nanoparticles for Intracellular Trafficking via Switchable Photoluminescence

Santosh K. Misra,[‡] Indrajit Srivastava,[‡] Indu Tripathi, Enrique Daza, Fatemeh Ostadhossein, and Dipanjan Pan*

Departments of Bioengineering, Beckman Institute, Materials Science and Engineering, Institute for Sustainability in Energy and Environment, University of Illinois at Urbana−Champaign, Urbana, Illinois 61801, United States

Mills Breast Cancer Institute, and Carle Foundation Hospital, Urbana, Illinois 61801, United States

Supporting Information

ABSTRACT: Reversible switching of photoluminescence (PL) of carbon nanoparticles (CNP) can be achieved with counterionic macromolecular caging and decaging at the nanoscale. A negatively charged uncoated, "bare" CNP with high luminescence loses its PL when positively charged macromolecules are wrapped around its surface. Prepared caged carbons could regain their emission only through interaction with anionic surfactant molecules, representing anionic amphiphiles of endocytic membranes. This process could be verified by gel electrophoresis, spectroscopically and *in vitro* confocal imaging studies. Results indicated for the first time that luminescence switchable CNPs can be synthesized for efficient intracellular tracking. This study further supports the origin of photoluminescence in CNP as a surface phenomenon correlated a function of characteristic charged macromolecules.

Carbon nanoparticles (CNPs) have recently been explored for multiscale imaging and therapeutic applications due to their intrinsic resistance to photobleaching, low toxicity, excellent biocompatibility and rather inexpensive large scale production.[1−8] Dissociative process of carrier and payload of nanomedicine in intracellular spaces have generally been studied by FRET and evaluated by functional activity, but direct evidence of payload delivery in case of CNPs requires a more sensitive and accurate technique. Switchable photoluminescence (PL) of CNPs with ability of upsurge in PL in intracellular spaces could be efficient strategy to follow the delivery of macromolecules or drugs passivated on CNPs. To make switchable CNPs, it is important to understand the origin of PL in CNPs so that a counter strategy can be used to quench the PL and regain it appropriately. However, a convincing explanations for origin of PL in CNPs is still lacking.[9] Among the four known PL principles,[10−14] the origin of surface based luminescence has been found to delegate optical as well as biological properties.[5,8,15−17] PL of quantum-confined electronic states of graphene oxide (GO) and photothermally reduced GO were found to be correlated with characteristics oxygen-containing functional groups,[18] and other surface functionalities but response to charge type and behavior correlation in CNP is yet to be revealed. In this work, we demonstrate that encapsulation ("caging") of bare-surface CNPs with positively charged cationic polymers leads to efficient PL quenching for bare CNPs. Interestingly, this quenching process is entirely reversible following a counterionic ligand interaction at the CNP nanoscale (Scheme 1).

Scheme 1. Schematic Representation of the Process of Preparing Luminescence Switchable CNPs Depicting Caging and Decaging by the Interaction of Counterionic Macromolecules

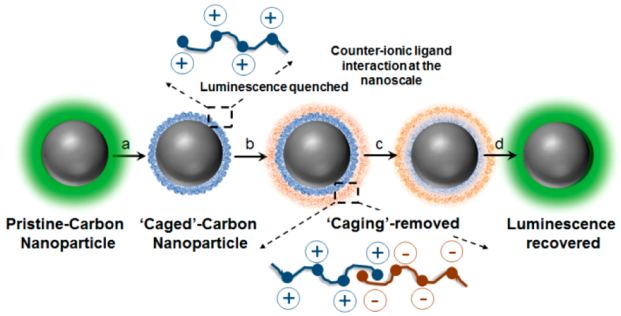

Reversible PL switch-ability can be verified by using three different types of cationic macromolecules i.e., branched polyethylenimine (PEI), polypeptidic poly L-lysine (polyLys) and dendritic poly amidoamine (PAMAM+) for caging of CNPs. The feasibility of "decaging" process can be confirmed using two different types of amphiphiles, anionic sodium dodecyl sulfate (SDS) and nonionic polyethylene glycolcetylether (PEGCE).

Initially, highly luminescent bare CNPs were prepared hydrothermally from a natural carbohydrate source (agave nectar).[19] As-synthesized CNPs were found to be 55 ± 5 nm in hydrodynamic diameter with a negative ζ-potential of −40 ± 6 mV (Figure 1). PEI wrapping resulted in a slightly bigger hydrodynamic diameter of 75 ± 9 nm. When the resultant PEI "caged" particles were incubated with SDS, formation of aggregated microstructures of ∼1100 nm was noticed likely due to the counterionic interaction at the nanoscale and freeing up of CNPs (Figure 1A). Interestingly, this observation was not noticed when caged-CNPs were postincubated with a non-anionic surfactant (i.e., PEGCE), presumably due to the lack of

Received: November 8, 2016
Published: January 20, 2017

DOI: 10.1021/jacs.6b11595
J. Am. Chem. Soc. 2017, 139, 1746−1749

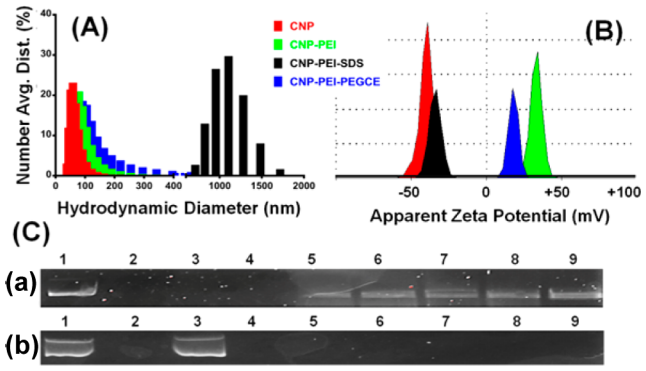

Figure 1. Physico-chemical characterization. Hydrodynamic diameter of CNPs at various stages of macromolecule-CNP interactions. (A) Size of pristine CNPs grew bigger with PEI passivation and further with SDS mediated PEI coagulations but did not change much with PEGCE incubations. (B) Change in ζ-potential of CNPs after incubation with PEI and further incubation with SDS or PEGCE. (C) Change in DNA interaction patterns postincubation with CNP-PEI in absence or presence of various concentration of SDS or PEGCE. (a) Lanes represent 1, DNA; 2, CNP; 3, DNA+PEI; 4, DNA +CNP-PEI; 5, DNA+CNP-PEI+SDS (5 M); 6, DNA+CNP-PEI+SDS (10 M); 7, DNA+CNP-PEI+SDS (15 M); 8, DNA+CNP-PEI+SDS (20 M); 9, DNA+CNP-PEI+SDS (25 M). (b) Lanes represent 1, DNA; 2, DNA+PEI; 3, DNA+CNP; 4, DNA+CNP-PEI; 5, DNA +CNP-PEI+PEGCE (5 M); 6, DNA+CNP-PEI+PEGCE (10 M); 7, DNA+CNP-PEI+PEGCE (15 M); 8, DNA+CNP-PEI+PEGCE (20 M); 9, DNA+CNP-PEI+PEGCE (25 M).

aggregation induced from counterionic interaction and showed a nonsignificant change in hydrodynamic sizes (Figure 1A). The anionic nature of SDS contributes to strong Coulombic interaction between PEI and SDS to generate aggregates whereas PEGCE, due to its nonionic nature did not produce any such aggregate. Use of polyLys and PAMAM+ as caging macromolecules did also show similar patterns but to a lesser extent, probably due to lower effective cationic charge on polyLys and PAMAM+ compared to PEI (abundance of 1°, 2° and 3° amines), which led to lower surface interaction and decaging by SDS molecules (Figure S1A–D).

This effect can also be noticed in ζ-potential patterns where negative ζ-potential of CNP (−40 mV) shifts to +35 mV with PEI caging and SDS incubation brings it back to −30 mV. The electrophoretic potential was not greatly influenced when PEGCE was used (+35 mV → +20 mV; Figure 1B). Interactions with PAMAM and polyLys with postincubation of SDS or PEGCE followed the same trend (Figure S2A,B). Furthermore, photoluminescent quantum yield (QY) values were calculated (Table S1) for CNP, CNP-PEI and CNP-PEI-SDS according to some previous reports[20,21] using Quinine sulfate as reference ($\varnothing$ = 0.54). It was observed that CNP had high QY value ($\varnothing$ = 0.23). However, "caging" the nanoparticle surface with PEI leads to a drastic drop in its QY value ($\varnothing$ = 0.02). Ultimately, on addition of anionic surfactant (SDS), pulls out PEI from the surface of the CNP, thereby clearing the CNP surface. This led the CNP to recover its emission to a very high extent as evident from its high QY value ($\varnothing$ = 0.21).

The process of CNP caging with positively charged passivating agents was also verified using gel electrophoresis with CNP, PEI and caged-CNP (CNP-PEI) in presence or absence of SDS, revealing information on ability of SDS to interact with surface-bound PEI. DNA was used as a secondary negatively charged biopolymer for competing interactions with positively charged molecules viz. PEI, against SDS. It was found that 200 ng of DNA could be retorted during gel electrophoresis by all the used PEI and CNP-PEI formulations (Figure S3). Here, lane 2 and 4 represent retarded DNA in the wells while free DNA, DNA complex with CNP and DNA-CNP complex incubated with SDS could show the free DNA in the gel as presented in lane 1, 2, and 7. While in case of lane 5 and 6 even use of high quantity of SDS (10 μL of 10M) could not release the plasmid DNA from DNA complex with PEI, likely due to insufficient amount of SDS and not all the used PEIs could complex with provided SDS. This in-turn did not release the DNA bound to PEI by competitive binding. Further experiments were performed to optimize SDS concentration where different amount of SDS was added to CNP-PEI-DNA complexes. All the used amounts of SDS (2, 4, 6, 8, and 10 μL of 50 M) could release DNA from the complex in an increasing order. This observation signifies the role of interaction of PEI-DNA interrupted by SDS leading to release of DNA during electrophoresis. This further confirmed the feasibility of reversible PEI caging and decaging on CNPs (Figure 1C-a). To establish if removal of PEI from CNP-PEIs involves the ionic interactions, an additional gel electrophoresis was performed using PEGCE replacing SDS (Figure 1C-b). As expected, at any of the added amount of PEGCE (equivalent to SDS amount,Figure 1C-b; i.e., 2, 4, 6, 8, and 10 μL (5, 10, 15, 20, or 25 M in lane 5–9, respectively) was not able to release DNA from CNP-PEI-DNA complex. Therefore, gel electrophoresis studies further confirmed the requirement of an ionic surfactant for freeing DNA from caged-CNPs. Raman spectroscopy based heat map imaging was performed to identify the chemical signatures and was successfully correlated with surface properties of CNPs. (Figure S4Ai–iii) Compositional characterization of CNPs was studied by multiple analytical and spectroscopic techniques including ^{1}H NMR (Figure S4B and Figure S5, S6), (Raman (Figure S8), FT-IR (Figure S9) and X-ray photoelectron spectroscopy (XPS) (Figure S10–S15) supporting the successful syntheses of the samples. UV–vis spectroscopic analysis revealed absorption maxima at λ_{max} ~ 300 nm (Figure S7). Interestingly, carbon particles are known to exhibit both the absorption and fluorescence patterns resembled to those of bandgap transitions typically found in nanoscale semiconductors and are affected with changing surface passivation's and chemistries.[22]

PL lifetime experiments were performed with CNP, CNP-PEI and CNP-PEI-SDS nanoparticles to reveal time-resolved decay profiles of the nanoparticles (Figure S16). All the samples including CNP, caged in PEI, polyLys or PAMAM+ and control samples were scanned over an excitation range of 300 to 800 nm and an emission range of 246 to 828 nm (Figure 2A). The process was further repeated with postincubation of SDS and PEGCE (Figure 2Aa–c and Figure 2Ad–f). Postprocessing of the emission data included inner-filtering correction with data obtained by simultaneous absorbance measurements and Rayleigh masking of signals produced because of light scattering of water. In addition, all emission intensities were normalized to a 1 mg/L quinine sulfate solution that was analyzed prior to each assay. As evident, PL of CNPs was decreased by caging with PEI and regained interaction with only anionic surfactant SDS (Figure 2Ac) but not with a nonionic surfactant (Figure 2Ae). To study the process of reversible switching of PL with macromolecular caging, further spectroscopic measurements were performed. All the caged nanoparticles exhibited a decrease in PL with PEI

DOI: 10.1021/jacs.6b11595
J. Am. Chem. Soc. 2017, 139, 1746–1749

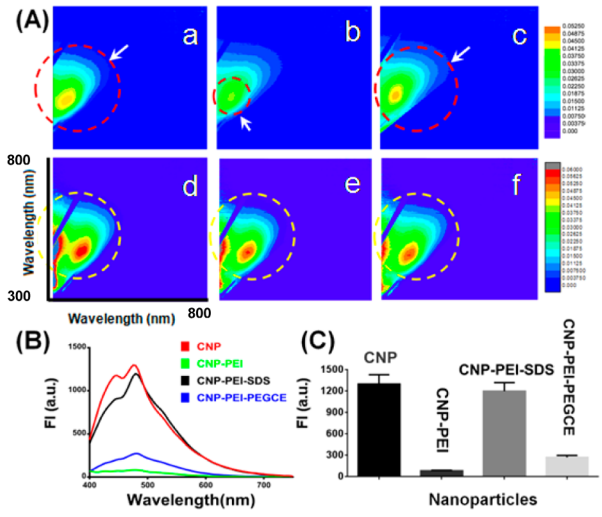

Figure 2. Emission studies on various CNP formulations post incubation with PEI, SDS or PEGCE sequentially. (A) Spectroscopic emission performed on (a, d) CNP; (b, e) CNP caged in PEI; (c) PEI caging removed from CNP using SDS and (f) PEI caging remained on CNP after use of PEGCE. Dotted circle indicates the loss and regain in PL of CNPs. *X* and *Y*-axes in all spectra show wavelength range 300 to 800 nm. (B, C) Emission spectra of CNP lowering the intensity post PEI caging and regains intensity after incubation with SDS whereas PEGCE incubation did not affect it to any considerable level.

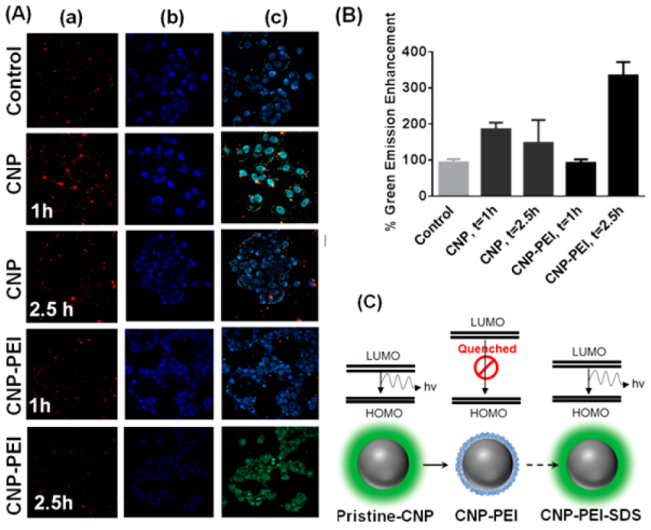

Figure 3. (A) Emission imaging on CNP and CNP-PEI formulations post incubation *in vitro*. MCF-7 cells were incubated with CNP and CNP-PEI (1 mg/mL) for 1 and 2.5h. Here a, b and c represent cell panels acquired under red (endosomal tracking dye), blue (DAPI in cell nucleus) and overlapped red and blue channels with green from CNPs. (B) Quantified PL from CNPs in MCF-7 incubated with formulations for different time points. (C) Schematic of plausible band gap diagram for the "caging" and "decaging" process.

caging (Figure 2B,C and Figure S17A–D). The order of decrease in PL postmacromolecular caging was found to be in order of PEI > Poly-Lys > PAMAM+ with value of ∼90, 70 and 40%, respectively (Figure S17E). Regaining of PL in CNP was achieved by SDS incubation (CNP-PEI+SDS) to a significantly high extent of ∼90% compared to ∼30% in both the cases of SDS incubated with CNP-polyLys and CNP-PAMAM+, respectively (Figure 2B, C and Figure S17E). The role of charged interactions on CNP surfaces in diminishing PL was also supported by PL regain only in case of anionic surfactant incubation (SDS) with no significant effect by nonionic PEGCE (Figure S17E). Similar patterns were achieved by spectral emission imaging experiments.

A colocalization with endosomal tracking dye (red channel, Figure 3Aa) confirmed the presence of CNPs within the intracellular space (Figure 3Ac) and seen interacting with endosomal membranes at longer time points. Results indicated unwrapping of cationic macromolecules from CNP-PEIs in situ at a longer incubation time point allowing stronger luminescence from free CNPs justifying the role of endosomal membranes interacting with PEI available on the surface of CNPs. This model system verified the role of cationic macromolecules on CNPs in delegating the level of PL in vitro. The PL switch-ability and trafficking of CNPs in an intracellular compartment was studied by confocal microscopy. Bare CNPs and CNP-PEIs (1 mg/mL) were incubated with breast cancer MCF-7 cells at 24 h (growth density of ∼80%) followed by fixing after 1 and 2.5 h of postincubation and imaged. A significantly low level of emission was seen in cells treated with caged-CNP-PEI samples compared to cells treated with bare CNPs at lower time point (1 h). Interestingly, CNPs were found to regain their luminescence at a longer time point (2.5h) (Figure 3B). A possible explanation for this behavior could be that at a longer time point, CNP-surface bound cationic branched macromolecular amines form complexes with anionic cellular lipids abundant in endosomal inner membranes, resulting in decaging of CNP-PEI delivered to cells. This process in turn results in a recovery of "masked" PL from CNPs.

A representative study on band gap of prepared CNPs (Figure 3C) was performed to understand the effect of "caging" and "decaging" phenomenon on CNP emission using Planck's quantum energy equation applied on absorption spectrum of CNPs. A low band gap value could be probable reason for allowing relatively easy absorption-emission transitions in CNP (ΔE = ∼2.63 eV). Interestingly, on tuning the nanoparticle surface with PEI, the ionic interactions between PEI and anionic surface of pristine CNP might have enhanced the band gap (ΔE = ∼3.12 eV), presumably due to the surface pacification[22] and thereby quenching its emission. However, once the PEI coating was removed by counterionic interactions with SDS, the band gap (ΔE = ∼2.70 eV) drops back to lower value allowing efficient absorbance-emission transitions, and consequently allowing the CNP to regain its original emission. Furthermore, the local polarity around CNPs may also dictate their photoluminescence properties.[23] Amines present on the nanoparticle surface modulate the local polarity.[24,25] The abundance of primary, secondary and tertiary amines on the surface of CNPs, may effectively reduce the local polarity at the nanoscale, thereby allowing the slower relaxation of solvent.[26] This might also lead to an inhomogeneous broad emission peak, which ultimately lowered the emission intensity. We postulate both of these processes are presumably contributing simultaneously to the cationic macromolecular-caging mediated drop in the observed CNP emission. The process of PL quenching was found to be significantly repeatable. (Figure S18A; I–V; B and C).

In conclusion, we demonstrated that reversible switching of photoluminescence of CNPs could be achieved efficiently with counterionic macromolecular "caging" and "decaging" at the nanoscale. This study further tries to delve mechanistically into

DOI: 10.1021/jacs.6b11595
J. Am. Chem. Soc. 2017, 139, 1746–1749

understanding the principle behind the origin of photoluminescence in CNP. Our results further supported that luminescence in CNPs are primarily a surface phenomenon[27,28] that can be reversibly turn on and off by a simple counterionic nanoscale chemistry. Our hypothesis was correlated as a function of characteristic charged macromolecules. A negatively charged uncoated, "bare" CNP with high luminescence loses its PL when positively charged macromolecules wrapped around the nanoscale surface. Non/-weakly luminescent caged carbons could regain their emission only through interaction with anionic surfactant molecules. This process could easily be applied in mammalian cells in vitro, where endocytic membrane abundant amphiphiles presumably represented anionic surfactants. This study indicated for the first time that luminescence switchable CNPs can be synthesized for efficient intracellular tracking.

■ ASSOCIATED CONTENT

Supporting Information

The Supporting Information is available free of charge on the ACS Publications website at DOI: 10.1021/jacs.6b11595.

Raman Imaging, ^{1}H NMR, additional gel electrophoresis image, UV−vis spectra, Raman spectra, FT-IR spectra, XPS survey and narrow scan spectra, PL life time spectra, additional emission spectra and quantification, Quantum yield calculation, Experimental details (PDF)

■ AUTHOR INFORMATION

Corresponding Author

*dipanjan@illinois.edu

ORCID

Dipanjan Pan: 0000-0003-0175-4704

Author Contributions

‡These authors contributed equally.

Notes

The authors declare the following competing financial interest(s): Prof Pan is the founder of three University based start-ups; however, these entities did not support this research.

■ ACKNOWLEDGMENTS

Funding support from the UIUC and Children's Discovery Institute are gratefully acknowledged. We thank Frederick Seitz Materials Research Laboratory, IGB and ISTC (O. Bojan), UIUC for analytical measurements. We thank J. A. N. T. Soares for PL lifetime experiment and Richard T. Haasch for XPS studies.

■ REFERENCES

(1) Baker, S. N.; Baker, G. A. *Angew. Chem., Int. Ed.* **2010**, *49*, 6726.
(2) Li, H. T.; Kang, Z. H.; Liu, Y.; Lee, S. T. *J. Mater. Chem.* **2012**, *22*, 24230.
(3) Zhu, S. J.; Tang, S. J.; Zhang, J. H.; Yang, B. *Chem. Commun.* **2012**, *48*, 4527.
(4) Shen, J. H.; Zhu, Y. H.; Yang, X. L.; Li, C. Z. *Chem. Commun.* **2012**, *48*, 3686.
(5) Misra, S. K.; Mukherjee, P.; Chang, H.-H.; Tiwari, S.; Gryka, M.; Bhargava, R.; Pan, D. *Sci. Rep.* **2016**, *6*, 29299.
(6) Tian, F.; Conde, J.; Bao, C.; Chen, Y.; Curtin, J.; Cui, D. *Biomaterials* **2016**, *106*, 87.
(7) Lin, P.; Cong, Y.; Zhang, B. *ACS Appl. Mater. Interfaces* **2015**, *7*, 6724.
(8) Misra, S. K.; Ostadhossein, F.; Daza, E.; Johnson, E. V.; Pan, D. *Adv. Funct. Mater.* **2016**, *26*, 8031.
(9) Cao, L.; Meziani, M. J.; Sahu, S.; Sun, Y. P. *Acc. Chem. Res.* **2013**, *46*, 171.
(10) Tao, H.; Yang, K.; Ma, Z.; Wan, J.; Zhang, Y.; Kang, Z.; Liu, Z. *Small* **2012**, *8*, 281.
(11) Zhou, B.; Lin, Y.; Wang, W.; Fernando, K. A.; Pathak, P.; Meziani, M. J.; Harruff, B. A.; Wang, X.; Wang, H.; Luo, P. G.; Yang, H.; Kose, M. E.; Chen, B.; Veca, L. M.; Xie, S. Y.; Sun, Y.-P. *J. Am. Chem. Soc.* **2006**, *128*, 7756.
(12) Liu, H.; Ye, T.; Mao, C. *Angew. Chem.* **2007**, *119*, 6593.
(13) Hola, K.; Bourlinos, A. B.; Kozak, O.; Berka, K.; Siskova, K. M.; Havrdova, M.; Tucek, J.; Safarova, K.; Otyepka, M.; Giannelis, E. P.; Zboril, R. *Carbon* **2014**, *70*, 279.
(14) Kwon, W.; Kim, Y.-H.; Lee, C.-L.; Lee, M.; Choi, H. C.; Lee, T.-W; Rhee, S.-W. *Nano Lett.* **2014**, *14*, 1306.
(15) Ostadhossein, F.; Misra, S. K.; Mukherjee, P.; Ostadhossein, A.; Daza, E.; Tiwari, S.; Mittal, S.; Gryka, M.; Bhargava, R.; Pan, D. *Small* **2016**, *12*, 5845.
(16) Misra, S. K.; Chang, H.-H.; Mukherjee, P.; Tiwari, S.; Ohoka, A.; Pan, D. *Sci. Rep.* **2015**, *5*, 14986.
(17) Mukherjee, P.; Misra, S. K.; Gryka, M.; Chang, H.-H.; Tiwari, S.; Wilson, W. L.; Scott, J. W.; Bhargava, R.; Pan, D. *Small* **2015**, *11*, 4691.
(18) Wang, L.; Wang, H. Y.; Wang, Y.; Zhu, S. J.; Zhang, Y. L.; Zhang, J. H.; Chen, Q. D.; Han, W.; Xu, H. L.; Yang, B.; Sun, H.-B. *Adv. Mater.* **2013**, *25*, 6539.
(19) Misra, S. K.; Mukherjee, P.; Chang, H.-H; Tiwari, S.; Gryka, M.; Bhargava, R.; Pan, D. *Sci. Rep.* **2016**, *6*, 29299.
(20) Sun, Y.; Shen, C.; Wang, J.; Lu, Y. *RSC Adv.* **2015**, *5*, 16368.
(21) Gu, J.; Hu, D.; Huang, J.; Huang, X.; Zhang, Q.; Jia, X.; Xi, K. *Nanoscale* **2016**, *8*, 3973.
(22) Wang, X.; Cao, L.; Yang, S.-T.; Lu, L.; Meziani, M. J.; Tian, L.; Sun, K. W.; Bloodgood, M. A.; Sun, Y.-P. *Angew. Chem., Int. Ed.* **2010**, *49*, 5310.
(23) Khan, S.; Gupta, A.; Verma, N. C.; Nandi, C. K. *Nano Lett.* **2015**, *15*, 8300.
(24) Sperling, R. A.; Parak, W. J. *Philos. Trans. R. Soc., A* **2010**, *368*, 1333.
(25) Wagner, N.; Theato, P. *Polymer* **2014**, *55*, 3436.
(26) Hutterer, R.; Schneider, F. W.; Lanig, H.; Hof, M. *Biochim. Biophys. Acta, Biomembr.* **1997**, *1323*, 195.
(27) Kwon, W.; Do, S.; Kim, J.-H.; Jeong, M. S.; Rhee, S.-W. *Sci. Rep.* **2015**, *5*, 12604.
(28) Li, X.; Zhang, S.; Kulinich, S. A.; Liu, Y.; Zeng, H. *Sci. Rep.* **2014**, *4*, 4976.

DOI: 10.1021/jacs.6b11595
J. Am. Chem. Soc. 2017, 139, 1746−1749